FHR Neutronics Benchmarking White Paper

April, 2016

UC Berkeley
Nuclear Engineering Department

Contents

List of Figures

List of Tables

1 Introduction

1.1 White paper outline

Fluoride-salt-cooled high-temperature reactors (FHRs) are a relatively new reactor concept, based on the combination of several existing reactor technologies. One of the greatest incentives behind developing FHRs is the promise of enhanced safety to existing reactor designs. The unique combination of engineering and materials present in an FHR allow for a high level of inherent passive safety, such as the ability of natural convection alone to sink enough decay heat via cooling towers to avoid post-scram meltdown. The fuel form of these salt-cooled reactors is a solid fuel employing the same tri-isotropic (TRISO) coated particles used in many high temperature gas-coolant reactors (HTGRs). There are a few different designs for fuel assemblies or elements, including pebbles, plates and prismatic blocks; this IRP focuses on a pebble-bed core design.

To date, no fueled experiments using pebbles immersed in salt have been conducted. This is further complicated by the inability to set up a simple experiment to obtain data about the neutronics behavior of such a system. Without a validation capability, early-stage benchmarking must rely heavily on code-to-code comparisons. Fortunately, as the pebble fuel has been used in critical facilities and reactor before, albeit not using a salt coolant, there are some measurement data available that capture some of the phenomena associated with the pebbles themselves, such as the so-called "double-heterogeneity" of the particle/pebble geometry. Reports from the International Atomic Energy Agency (IAEA) Collaborative Research Projects (CRPs) such as IAEA-TECDOC-1382 and IAEA-TECDOC-1694 contain a great deal of information and benchmark data from various HTGR facilities and verification scenarios. Of particular interest to the IRP at this stage is the Pebble-Bed Modular Reactor (PBMR) "Pebble Box" benchmark in IAEA-TECDOC-1694, which defines a number of test cases for the purposes of a code capabilities check. The design of test cases for the IRP FHR neutronics benchmark are very similar to the Pebble Box benchmark, both of which start with a simple, infinite cell containing pebbles and is examined with varying levels of homogenization. This allows some quantification of the resonance self-shielding and neutron streaming effects. The second scenario includes a graphite reflector and black boundaries to simulate a simplified reactor geometry, allowing for leakage and reflector effects.

Section 2 of this report contains the details of the neutronics benchmark specification completed to date with reference results calculated using Serpent 2. Section 3 contains information on the baseline comparison of results between candidate codes for FHR analysis.

1.2 FHR neutronics from the second IRP

A second IRP lead by the Georgia Institute of Technology is investigating, in parallel with this IRP, FHR systems using a different fuel form, namely plate-type fuel. As part of the scoping analysis for the research, they have conducted a Phenomena Identification and Ranking Table (PIRT)-like exercise to establish the important neutronic phenomena of interest when designing FHRs. As most neutronics codes were developed and optimized for light-water reactor (LWR) simulation, it is important to establish the level of fidelity that a given code can achieve when simulating an FHR.

As a result of a meeting in December 2015, figures of merit (FOM) and important phenomena were identified for analysis in FHR benchmarking exercises. The FOM identified were simply the

multiplication factor and plate fission density. The phenomena identified were moderation, thermalisation and absorption in flibe and thermalisation and absorption in graphite.
It is likely that although the two IRPs are dealing with different fuel geometries, there will be overlap of scope that will allow a sharing of resources and experience.

2 Benchmark specification

2.1 Unit cell benchmark specification

2.1.1 Introduction

This benchmark focuses on the neutronics physics behavior of a Face-Centered Cubic (FCC) unit cell system. The main concern of the study is to test code capabilities and to make a code-to-code comparison. We would also like to investigate the reasons for any difference in results from different codes. The enrichment of Li-7 in FLiBe is set to 99.99% in this calculation. However, Li-7 enrichment in later version of this benchmark will be increased to 99.995%. Here we only provide results with 99.99% Li-7 enrichment.

2.1.2 Case specification

The unit cell benchmark consists of three cases:

Case 1: Homogenous mixture

Description: Case 1 is a cubic unit cell filled with one single material that is a mixture of coolant and all the pebble components.

Geometry: The side length of the cube is 9.2575 cm, with reflective boundary conditions on all sides.

Material:

Table 1 Material information for Case 1

Material	Density, g/cm^3	Temperature, K	Isotope	Mass fraction	Atom fraction
Mixture	1.872	900	O-16	2.53927E-03	
			U-235	3.22769E-03	
			U-238	1.56268E-02	
			C-nature	5.20535E-01	
			Si-nature	4.82195E-03	
			B-10	4.63687E-08	
			B-11	2.06506E-07	
			Li-6	5.50568E-06	
			Li-7	6.42115E-02	
			Be-9	4.12446E-02	
			F-19	3.47787E-01	

Cross sections: Participants can use cross section data from any library. Whether or not using graphite scattering kernel for carbon is optional.

Case 2: Single level heterogeneity

Description: Case 2 is a cubic unit cell filled with pebbles and coolant. The pebbles are comprised of a homogeneous inner fuel region and shell.

Geometry: The side length of the cube is 9.2575 cm, with reflective boundary conditions on all sides. As shown in Figure 1, there are eight 1/8 pebbles in the vertex, six 1/2 pebbles in the face center of the cube. The radius of pebble is 3 cm and the radius of its inner fuel region is 2.5 cm. The space among pebbles is filled with FLiBe coolant.

Material:

Table 2 Material information for Case 2

Material	Density, g/cm^3	Temperature, K	Isotope	Mass fraction (relative)	Atom fraction (relative)
Fuel	1.842	900	O-16	7.81961E-03	
			U-235	9.93958E-03	
			U-238	4.81225E-02	
			C-nature	9.19269E-01	
			Si-nature	1.48491E-02	
			B-10	8.01063E-08	
			B-11	3.56758E-07	
Matrix (shell)	1.73	900	C-nature		8.77414E-02
			B-10		9.64977E-09
			B-11		3.90864E-08
FLiBe	1.9740	900	Li-6		0.0002
			Li-7		1.9998
			Be-9		1.0000
			F-19		4.0000

Cross sections: Participants can use cross section data from any library. Whether or not using graphite scattering kernel for carbon is optional.

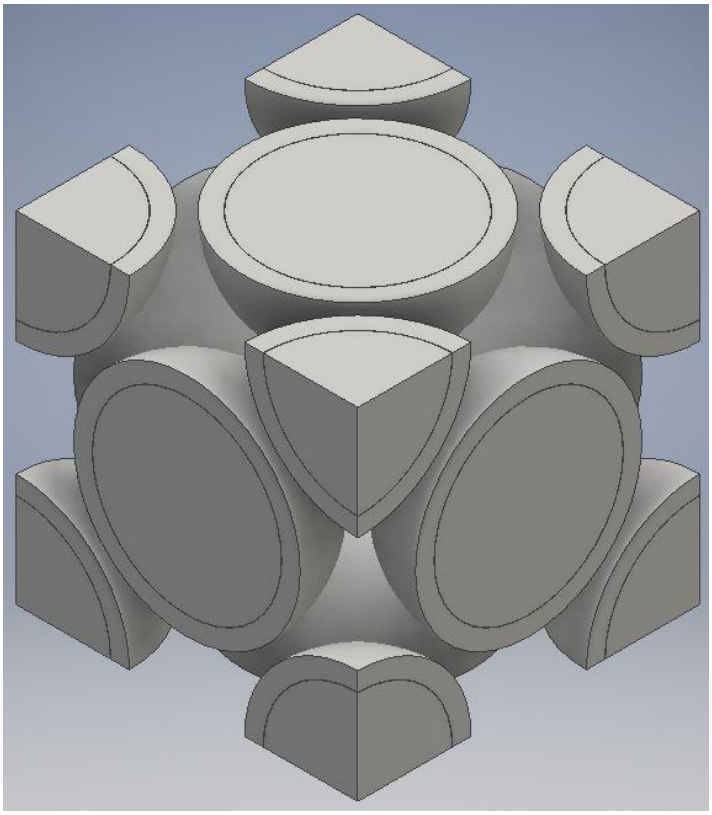

Figure 1 Case 2 configuration

Table 3 Case 2 geometry information

Packing fraction	57.02%
Radius of the pebble	3cm
Radius of inner fuel region	2.5cm
Thickness of shell	0.5cm

Case 3: Double heterogeneity

Description: Case 3 is a cubic unit cell filled with pebbles and coolant. The pebbles are comprised of an inner fuel region and shell. The inner fuel region of pebble is comprised of 11558 fuel particles and graphite matrix. The packing factor of fuel particles is 6.97%.

Geometry: The side length of the cube is 9.2575 cm, with reflective boundary conditions on all sides. Case 3 keeps everything the same as case 2 except that the inner fuel region of pebble is filled with particles and graphite matrix as shown in Figure 2. The radius of fuel particle is 0.0455 cm. For the ordered particles, the side length of particle FCC lattice is 0.2828 cm.

Table 4 Case 3 TRISO geometry information

Centre fuel kernel radius	0.025 cm
Buffer layer thickness	0.009 cm
Inner PyC layer thickness	0.004 cm
SiC layer thickness	0.0035 cm
Outer PyC layer thickness	0.004 cm
Particle radius	0.0455 cm

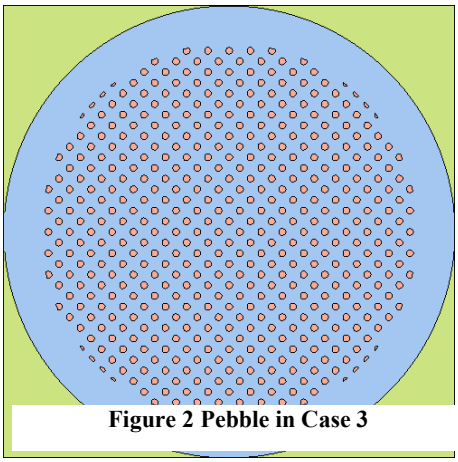

Figure 2 Pebble in Case 3

Material:

Table 5 Material information for Case 3

Material	Density, g/cm^3	Temperature, K	Isotope	Mass fraction (relative)	Atom fraction (relative)
Fuel	10.5	900	O-16		2.0
			U-235		0.173
			U-238		0.827
Buffer	1.05	900	C-nature		1
PyC	1.90	900	C-nature		1
SiC	3.18	900	Si-nature		4.77240E-02
			C-nature		4.77240E-02
Matrix (shell)	1.73	900	C-nature		8.77414E-02
			B-10		9.64977E-09
			B-11		3.90864E-08
FLiBe	1.9740	900	Li-6		0.0002
			Li-7		1.9998

			Be-9		1.0000
			F-19		4.0000

Cross sections: Participants can use cross section data from any library. Whether or not using graphite scattering kernel for carbon is optional.

2.1.3 Results of interest

The following results should be provided in all three cases:

a. K-eff
b. Effective delayed neutron fraction
c. Effective generation time & life-time
d. Homogenized neutron spectrum
e. Selected cross section in case 3 (shown in Table 6)

Table 6 Expected cross section

Li-6	(n, t)
Li-7	Capture
F	Capture
U-238	Capture
U-235	Fission
U-235	Capture
FLiBe	Elastic scattering

2.1.4 Reference result

2.1.4.1 Software used

Here we use Serpent – 3D Monte Carlo code to calculate the reference result.

2.1.4.2 Case 1&2&3 using thermal scattering cross sections for carbon

According to Table 7 and Table 8, no matter using thermal scattering library or not, the k-eff values will increase when taking heterogeneity into account. For case 3, we also perform a calculation with random TRISO distribution and the k-eff will be greater than that with ordered TRISO. The difference is mainly from the cut-off effect in ordered TRISO distribution.

Table 7 Summarized results using thermal scattering library

	case1		case2		case3(ordered TRISO)		case3(random TRISO)	
k-eff	1.30504E+00	3.4E-05	1.34638E+00	3.5E-05	1.42187E+00	3.7E-05	1.42516E+00	3.7E-05
beta_eff	6.51083E-03	0.00089	6.50994E-03	0.00087	6.48759E-03	0.00083	6.50227E-03	0.00083
gen_time	2.88459E-04	0.00011	2.83159E-04	0.00011	2.74491E-04	0.00011	2.74415E-04	0.00011
lifetime	3.76446E-04	7.4E-05	3.81189E-04	7.3E-05	3.90265E-04	6.8E-05	3.91036E-04	7.0E-05

2.1.4.3 Case 1&2&3 not using thermal scattering cross sections for carbon

Table 8 Summarized results not using thermal scattering library

	case1		case2		case3(ordered)	
k-eff	1.30685E+00	3.4E-05	1.34900E+00	3.5E-05	1.42435E+00	3.7E-05
beta_eff	6.51428E-03	0.00087	6.55570E-03	0.00088	6.52010E-03	0.00084
gen_time	2.87402E-04	0.00012	2.81364E-04	0.00011	2.73186E-04	0.00011
lifetime	3.75592E-04	7.5E-05	3.79505E-04	7.1E-05	3.89049E-04	7.1E-05

2.1.4.4 Neutron spectrum

Figure 3 shows the average normalized flux in different cases with 238 energy groups. In cases with higher heterogeneity level, the thermal flux will be larger.

Figure 4 shows the normalized flux in different regions of case 3. The thermal flux in fuel region will be smaller than that in other two regions.

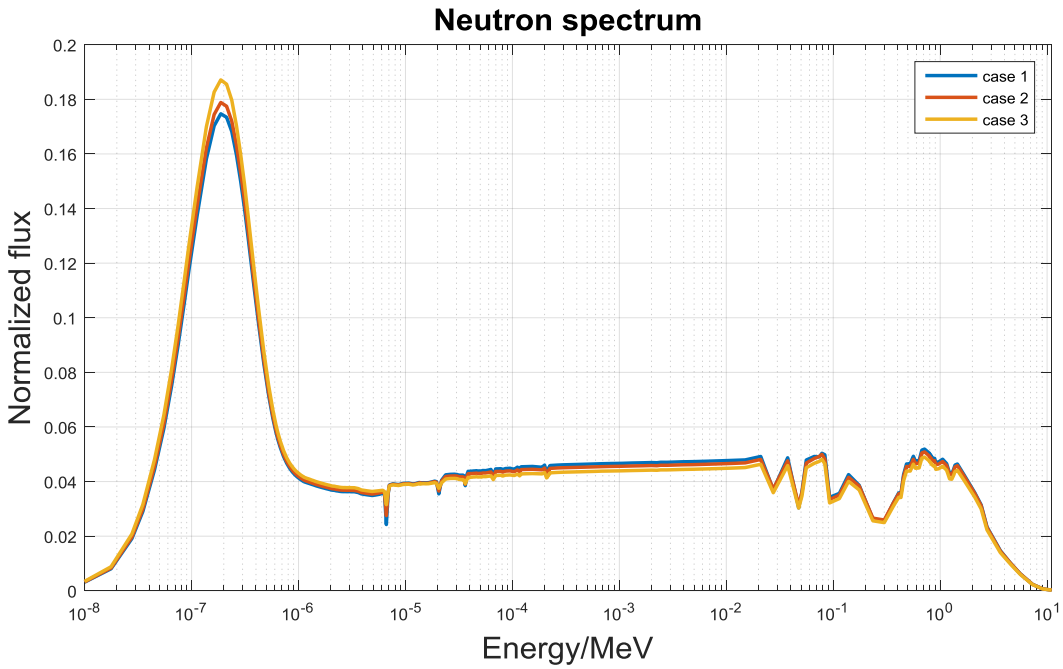

Figure 3 Average neutron spectrum in Scale238 energy grid

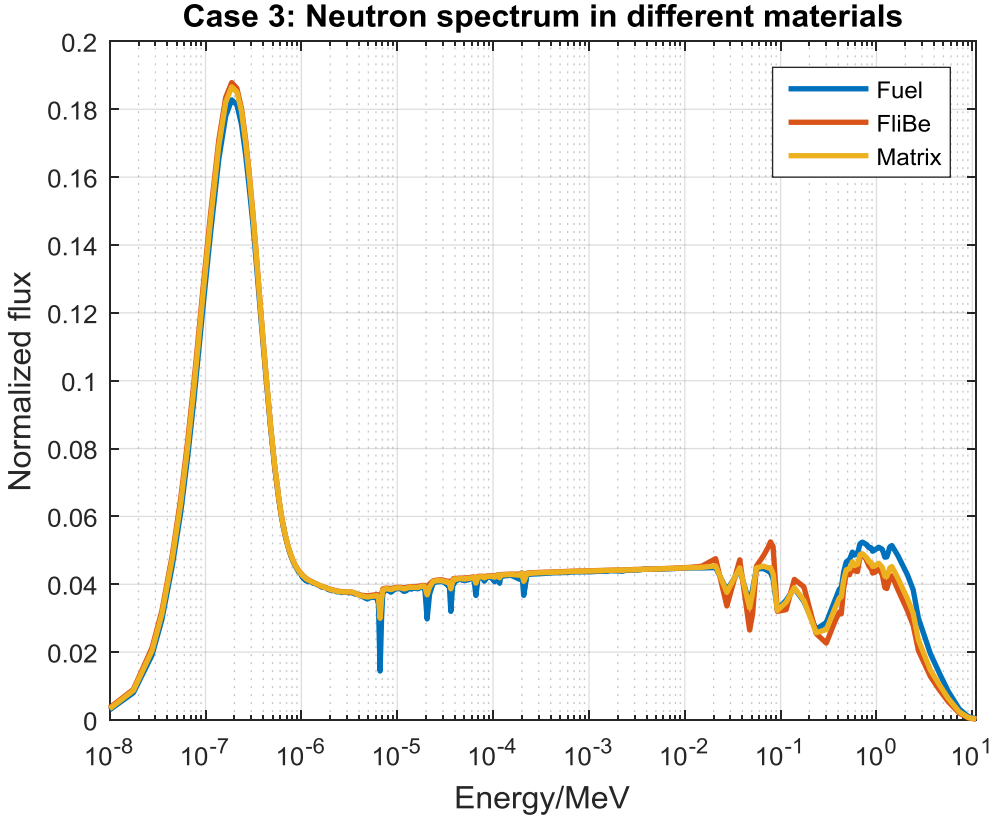

Figure 4 Case 3: Neutron spectrum in different materials

2.1.4.5 Selected cross section

In certain energy group, microscopic cross section can be expressed as:

$$\sigma = \frac{\Sigma[\mathrm{cm}^{-1}]}{N[\mathrm{cm}^{-1}\cdot \mathrm{b}^{-1}]} = \frac{1}{N}\frac{\int_V \int_{E_{i+1}}^{E_i} \Sigma(\mathrm{r},\mathrm{E})\phi(\mathrm{r},\mathrm{E})\,\mathrm{d}^3\, rdE}{\int_V \int_{E_{i+1}}^{E_i} \phi(\mathrm{r},\mathrm{E})\,\mathrm{d}^3\, rdE}$$

Table 9 and Table 10 show the selected microscopic and macroscopic cross sections.

Table 9 4-group microscopic cross section

Energy group, MeV	Microscopic cross section ,b					
	Li-6(n, t)	Li-7(n, γ)	F(n, γ)	U-238(n,γ)	U-235(n,f)	U-235(n,γ)
[1.00000E-11, 6.25000E-07]	4.22843E+02	2.03609E-02	4.29247E-03	1.21090E+00	2.31901E+02	4.23222E+01
[6.25000E-07, 5.53000E-03]	4.09470E+01	1.97733E-03	4.20312E-04	1.14476E+01	2.66002E+01	1.39338E+01
[5.53000E-03, 8.21000E-01]	1.03750E+00	4.74510E-05	1.03526E-03	3.57175E-01	1.93451E+00	5.82802E-01
[8.21000E-01, 1.00000E+01]	2.06658E-01	4.83508E-06	1.00440E-04	6.52802E-02	1.21795E+00	6.89562E-02

Table 10 FLiBe elastic scattering macroscopic cross section

Energy group, MeV	Macroscopic cross section, cm^{-1}
[1.00000E-11, 6.25000E-07]	2.79699E-01
[6.25000E-07, 5.53000E-03]	2.74905E-01
[5.53000E-03, 8.21000E-01]	3.22302E-01
[8.21000E-01, 1.00000E+01]	1.73396E-01

2.2 3D full core benchmark specification

2.2.1 Introduction

Based on TMSR-SF1 core, 3D full core benchmark is performed on a solid fuel molten salt cooled high-temperature reactor. It uses 6.0cm-diamter spherical fuel elements which contains 17.12wt% uranium. The coolant of primary loop is 2LiF-BeF_2 molten salt. The temperature is set to 900 K.

2.2.2 Core layout

The cylinder core includes a middle cylinder active region, top reflector, bottom reflector and radial reflector as shown in Figure 5 and detailed parameters can be found in Table 11. The top and bottom reflector are mixture of graphite and coolant. For the top reflector, the volume ratio of FLiBe and graphite is 1:3.69936 and for the bottom reflector, the volume ratio of FLiBe and graphite is 1:3.08061. The active region consists of a fuel region and a pure coolant region. Fuel pebbles are distributed randomly in the fuel region which is the upper section of active core. In later calculation, the pebble distribution is assumed as FCC ordered. The gap among pebbles and the bottom section of active core are filled by coolant.

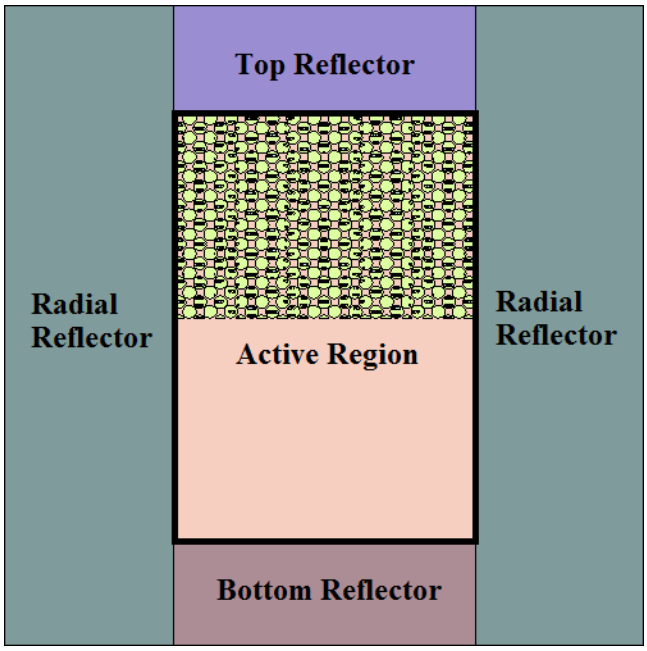

Figure 5 Layout of the core

Table 11 Parameter of core design

Active region	
The diameter/height of the active region	135cm/205.7cm
The height of fuel region	99.3223 cm
The packing factor of fuel region	57.02%
Temperature	900K
Reflector layer	
The diameter/height of the top reflector	135cm/50.35cm
The diameter/height of the bottom reflector	135cm/50.35cm

The outer shape of radial reflector	Cylinder, diameter: 285.0cm, height: 306.4cm

2.2.3 Fuel elements

The core uses 6.0 cm-diameter spherical pebble fuel elements. Each pebble contains 11558 TRISO particles. Graphite is used to fill the gap among fuel particles and to compose the cladding of pebble. The design parameter of pebbles is shown in Table 12.

Table 12 Design parameter of fuel pebble element

Radius of the pebble	3cm
Radius of inner fuel region	2.5cm
Thickness of shell	0.5cm

The design parameter of TRISO is as follows:

Table 13 Design parameter of TRISO

Centre fuel kernel radius	0.025 cm
Buffer layer thickness	0.009 cm
Inner PyC layer thickness	0.004 cm
SiC layer thickness	0.0035 cm
Outer PyC layer thickness	0.004 cm
Particle radius	0.0455 cm

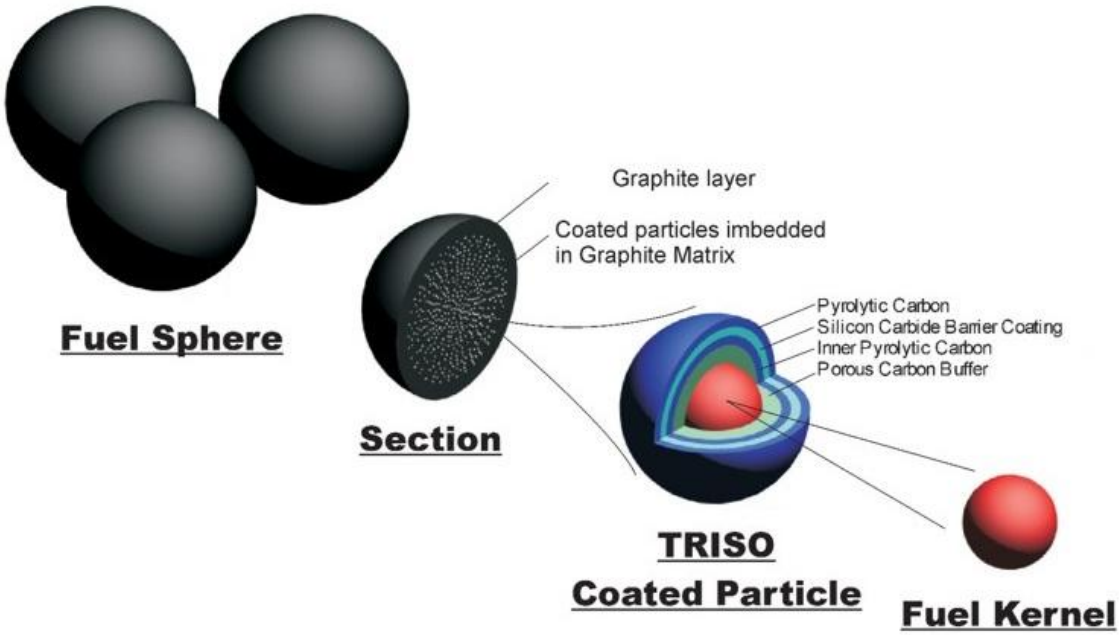

Figure 6 Fuel element

2.2.4 Material

The material data for fuel elements can be found in Table 14.
The density of FLiBe is calculated by the following formula where the unit of temperature T is C:

$$\rho = 2279.92 - 0.488 \cdot T(kg/m^3)$$

Table 14 Fuel element material

Fuel region in TRISO	Total mass density = 10.5 g/cm^3
Isotope	Relative atom density
O-16	2.0
U-235	0.173
U-238	0.827
Buffer layer	Total mass density = 1.05 g/cm^3
C	1
PyC layer	Total mass density = 1.90 g/cm^3
C	1
SiC layer	Total mass density = 3.18 g/cm^3
Isotope	Relative atom density
Si	4.77240E-02
C	4.77240E-02
Matrix (shell) of pebble	Total mass density = 1.73 g/cm^3
Isotope	Relative atom density
C	8.77414E-02
B-10	9.64977E-09
B-11	3.90864E-08

Table 15 and Table 16 list the material data for coolant FLiBe and graphite reflector.

Table 15 Coolant material

FLiBe	Total mass density = 1.9740 g/cm^3
Isotope	Relative atom density
Li-6	0.0002
Li-7	1.9998
Be-9	1.0000
F-19	4.0000

Table 16 Graphite reflector material

Radial reflector	Total mass density = 1.75 g/cm^3
Isotope	Relative atom density
C	8.77414E-02
B-10	9.64977E-09
B-11	3.90864E-08
Upper reflector	Total mass density = 1.7977 g/cm^3
Isotope	Relative mass density

C	1.3776
B-10	1.2630E-07
B-11	5.6251E-07
Li-6	5.1025E-06
Li-7	5.9509E-02
Be-9	3.8224E-02
F-19	3.2232E-01
Bottom reflector	Total mass density = 1.8049 g/cm^3
Isotope	Relative mass density
C	1.32114
B-10	1.21128E-07
B-11	5.3945E-07
Li-6	5.8762E-06
Li-7	6.8533E-02
Be-9	4.4020E-02
F-19	3.7119E-01

2.2.5 Results of interest

The following results should be provided:

a. K_{eff}
b. Neutron spectrum (average flux in the fuel region of kernel)
c. Radial Leakage and axial leakage
d. Peaking factor (axial peaking factor & radial peaking factor)
e. Several locations: power flux spectrum (scale238)
f. Prompt lifetime
g. Effective generation time ADJ
h. Beta effective(effective delayed neutron fraction)
i. Reactivity coefficients
j. With/without alpha beta to see the k-eff and spectrum

2.2.6 Reference result

2.2.6.1 Face-Centered Cubic lattice design

For FCC ordered pebbles and particles, we need to define the pitch length of FCC lattice. From Table 17, we can conclude that the optimal pitch length for TRISO and pebble lattice are 0.2828 cm and 9.25 cm.

Table 17 FCC lattice design

Pitch of TRISO lattice (cm)	packing factor	Designed packing factor: 6.9678%
0.2829	6.95%	
0.2828	6.97%	
Pitch of pebble lattice (cm)	packing factor	Designed packing factor: 57.02%
9.24	57.21%	
9.25	57.03%	
9.2575	56.90%	

9.26	56.85%	

The center of pebble FCC lattice is located in the center of fuel region.

2.2.6.2 Software used

Here we use Serpent – 3D Monte Carlo code to calculate the reference result.

2.2.6.3 Summarized results

According to Table 18, k-eff with TSL will be smaller than that without TSL.

Table 18 Summarized results (1)

	Ordered pebbles and particles				Random pebbles and particles	
	Using thermal scattering libraries		Not using thermal scattering libraries			
Keff	9.93376E-01	8.3E-05	9.98900E-01	8.4E-05	1.00065E+00	8.4E-05
Generation time	6.66765E-04	0.00019	6.70006E-04	0.00019	6.39128E-04	0.00019
Lifetime	6.66980E-04	0.00028	6.74203E-04	0.00029	6.44081E-04	0.00029
Prompt lifetime	6.67134E-04	0.00028	6.74359E-04	0.00029	6.44243E-04	0.00029
Beta effective	6.77814E-03	0.00111	6.77636E-03	0.00109	6.76688E-03	0.00108

As shown in Table 19, more neutron leakage will be found in the radial direction. The leakage from bottom surface is the smallest.

Table 19 Summarized results (2)

Leakage from the outer cylinder	Radial leakage	11.46%
	Upper leakage	5.64%
	Bottom leakage	0.16%
Axial peaking factor		1.1556
Radial peaking factor		1.1497

Table 20 shows the value of Doppler coefficient, coolant temperature coefficient and void reactivity coefficient. They are all negative according to the calculation.

Table 20 Summarized results (3)

Doppler coefficient	900K		1200K		$\Delta\rho$(pcm)	$\Delta\rho/\Delta T$
	Keff=0.993376	8.3E-05	Keff=0.986853	8.3E-05	-665.40±11.74	-2.2180±0.0391
Coolant temperature coefficient	900K (ρ=1.9740g/cm3)		1200K (ρ=1.8276g/cm3)		$\Delta\rho$(pcm)	$\Delta\rho/\Delta T$
	Keff=0.993376	8.3E-05	Keff=0.988471	8.3E-05	-499.53±11.74	-1.6651±0.0391

Void reactivity coefficient	Void fraction = 0%		Void fraction = 5% (ρ=1.8753g/cm3)		$\Delta\rho$(pcm)	$\Delta\rho/\Delta$void fraction
	Keff=0.993376	8.3E-05	Keff=0.992830	8.3E-05	-55.36±11.74	-11.07±2.35

Figure 7 compares the neutron spectrum in fuel region in two calculations. The thermal flux fraction will be larger in the case with thermal scattering library.

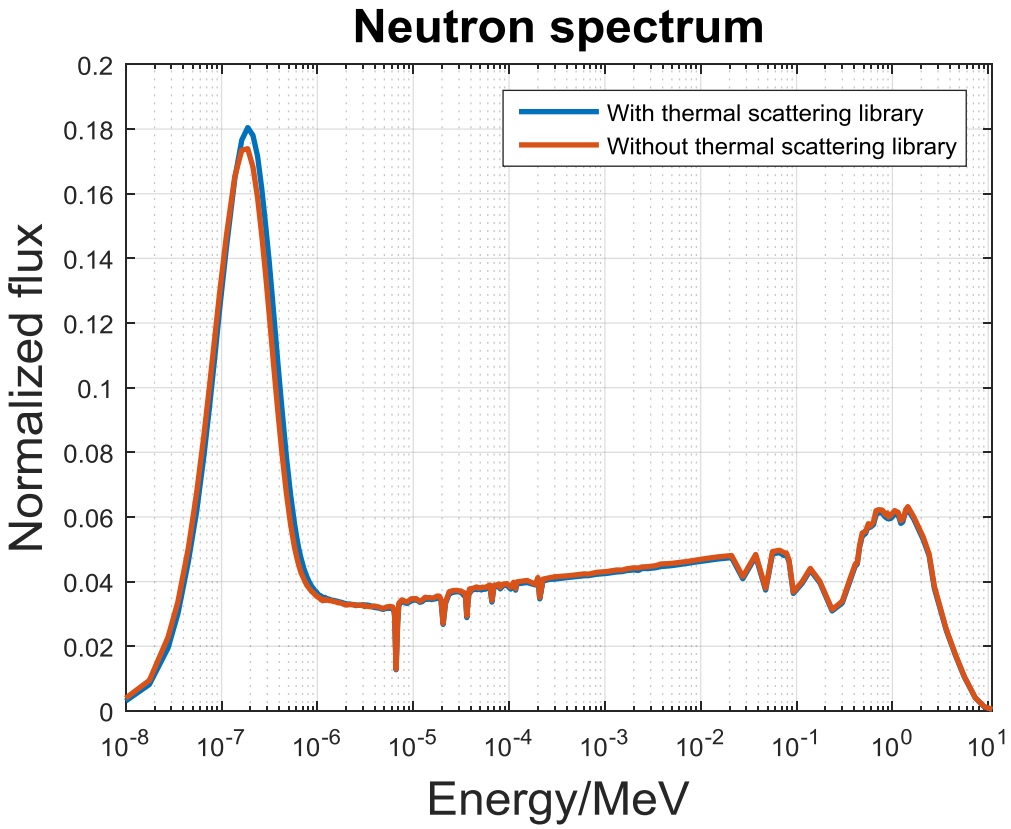

Figure 7 Neutron spectrum in fuel region of kernel

Figure 8 and Figure 9 show the thermal flux in X-Y plane and X-Z plane. There are clearly peaks in thermal flux in the region near reflector. Figure 10 and Figure 11 also prove this conclusion.

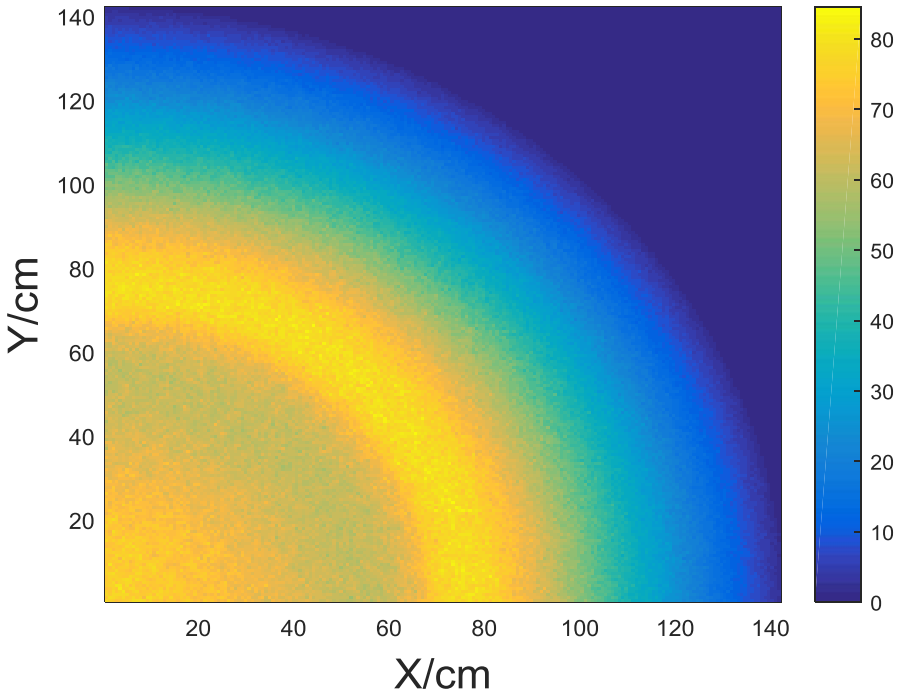

Figure 8 Thermal flux in X-Y plane

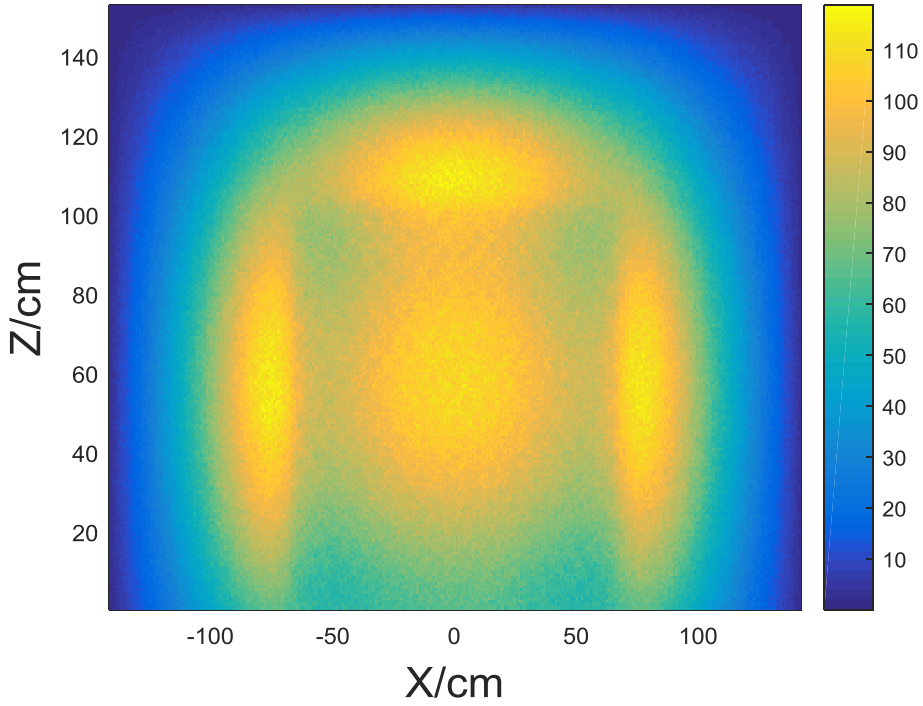

Figure 9 Thermal flux in X-Z plane

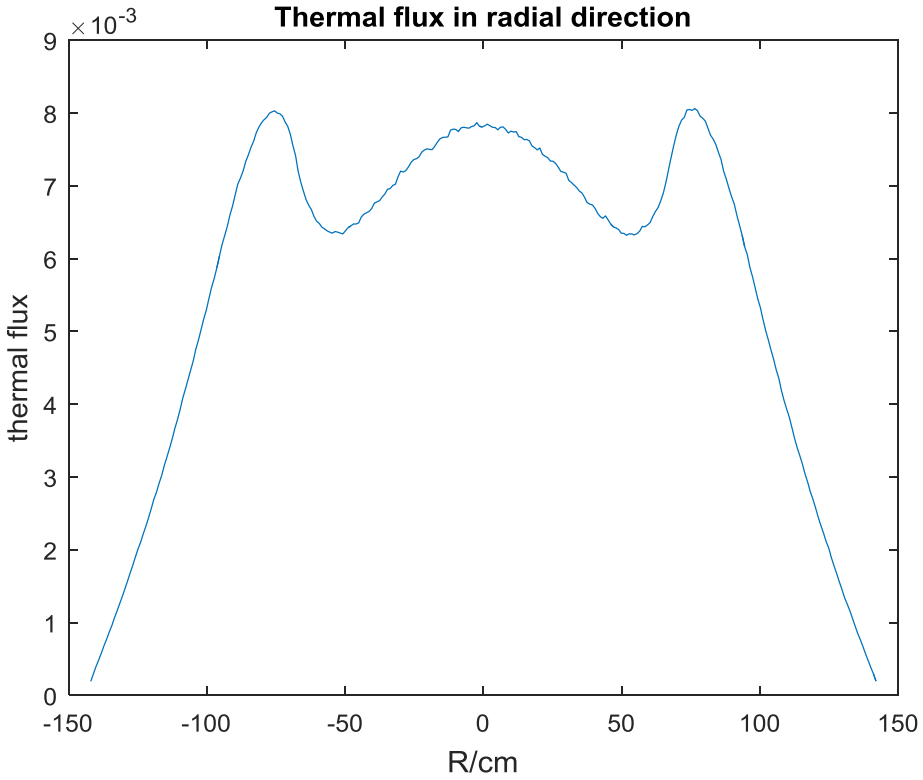

Figure 10 Radial thermal flux integrated from Z=3.5277 to Z=102.85cm

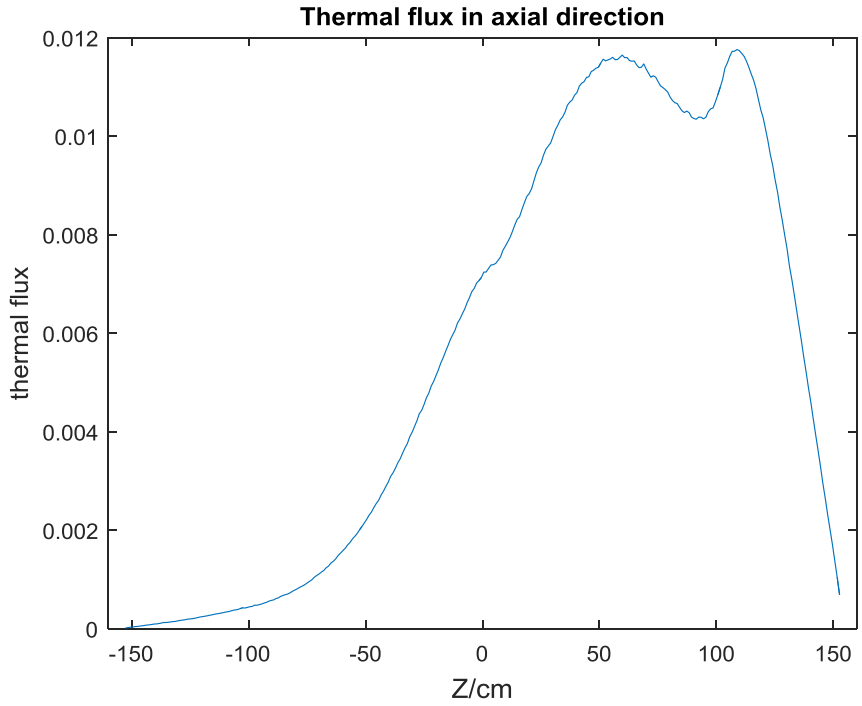

Figure 11 Axial thermal flux integrated from X=-67.5 to X=67.5cm

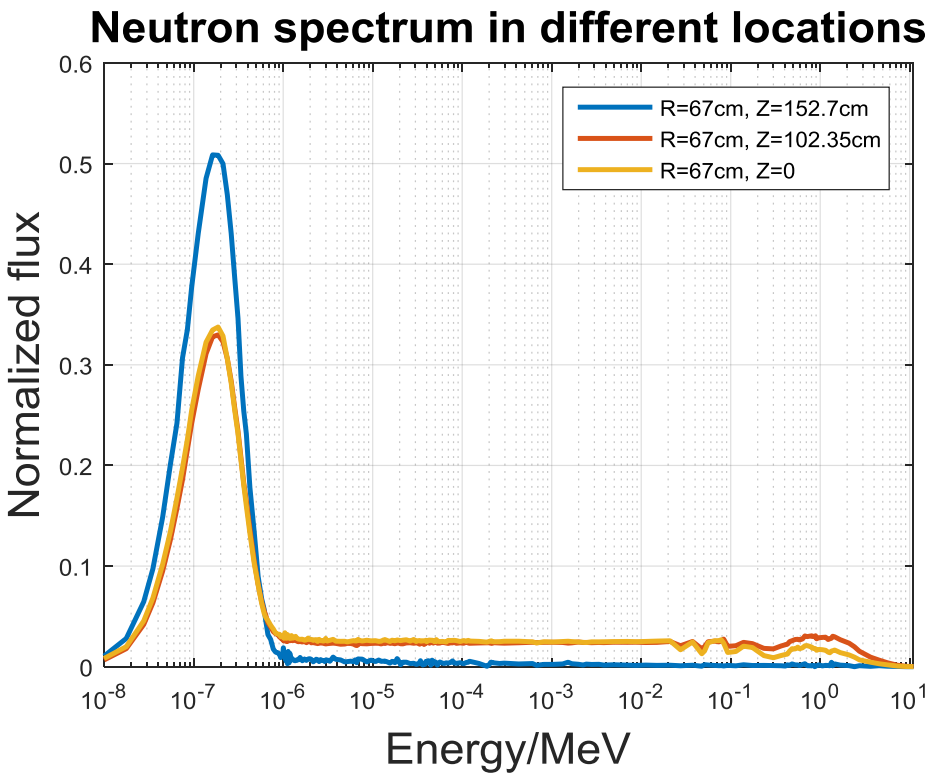

Figure 12 Neutron spectrum in different locations

Figure 12 shows the normalized neutron spectrum in different locations. In the outer surface of the top reflector, the thermal flux fraction is pretty larger than that in the active region.

3 Code-to-code comparison results

Identification of modelling issues and other simulation phenomena is important in developing a robust benchmark specification. The is important to code effects from the methodological effects; it is important that the specification describes a system that does not leave a great deal of ambiguity in its details that can lead to errors in simulations results separate to differences in calculated values arising from different codes. The latter is one of the key outcomes of this benchmark, while the former serves only to add unnecessary error in the comparison.

3.1 Codes used in baseline comparison

There are a number of neutronics codes available to perform criticality simulations, calculate fluxes, generate cross-sections, perform sensitivity analyses, burnup and generate point-kinetic parameters. There are two primary methodological approaches to solving these problems: deterministic and stochastic. While the deterministic approach is more mature and even preferred by many to perform neutronics calculations, the stochastic approach offers a higher-fidelity simulation by avoid a number of approximations necessary to perform the necessary calculations. This benchmarking exercise not only provides the opportunity to use both and compare results but may uncover certain issues that arise from using either methodology; it is thought that Monte Carlo codes, the principle stochastic approach, is better suited to TRISO/pebble fuels, owing to the high-fidelity between the geometry definition in a model and the physical reality of a system. However, it lacks the historical confidence that deterministic codes now enjoy as well as suffering from an increased computational demand.
This work within this report shows the preliminary work done using the following codes and methodologies:

- Serpent, a 3D criticality/burnup Monte Carlo code from VTT, Finland.
- MCNP6, 3D general-purpose Monte Carlo transport code from LANL, US.
- SCALE6.1, a simulation suite designed for nuclear safety analysis with dozen of purpose-built modules for various applications, developed at ORNL, US. The transport modules within SCALE6.1 used are:
    - T-XSDRN, a 1D discrete ordinates code used in the TRITON sequence.
    - KENO-VI, a 3D Monte Carlo code.

3.1.1 Serpent (3D Monte Carlo)

This code allows for the explicit modelling of the whole geometry in the DH scenario with far fewer approximations than deterministic codes use. Serpent features capability to model particle/pebble fuel in several ways, including a per-particle co-ordinate location and full coating geometry.

3.1.2 MCNP6 (3D Monte Carlo)

MCNP6 is a general-purpose transport code used for neutron, electron and photon transport problems. It is very flexible, capable of modeling the DH systems of FHRs

3.1.3 SCALE – T-XSDRN (1D Discrete Ordinates)

This simulations obtained from this module constitute the deterministic side of this work. As the code is 1D, the model for cases 2 and 3 have been adapted as described in the 1D Model section. The single and double heterogeneity are handled by using a cross-section treatment to calculate the flux disadvantage factors of the fuel cell.

3.1.4 SCALE – KENO-VI (3D Monte Carlo)

KENO-VI is a similar code to Serpent and provides the transport for a number of sequences with SCALE. While Serpent is likely more suited for analysis of pebble fuel, KENO-VI is still a Monte Carlo code and also shares many of the pre/post modules with T-XSDRN, as well as using a standardized geometry input generated for all SCALE modules. By using KENO-VI, it is hoped some bridge between the use of Serpent and T-XSDRN can be realized. Also, KENO-VI can use both a continuous energy and multi-group energy cross section library.

3.2 Iterative benchmark specification design process

One of the major challenged of developing a benchmark is defining a scenario for participants to model that is succinct, clear, without error, well-defined, but not overly constrained. It's important to strike a balance between providing a detailed benchmark with as few degrees of freedom as possible to limit sources of error between participants' results, yet providing enough scope for users to implement the parameters of the specification into their model within the limits of their nominated code capabilities. This was a topic that was discussed at some length during the April 2016 meeting, particularly when trying to accommodate the limitations from deterministic codes. It was generally agreed that erring on the side of user freedom is the best approach. This does necessitate a rigorous reporting system that prompts participant to provide details on their methods for dealing with approximations not specified in the benchmark. For example, the issue of providing cross-sections was broached for participants electing to use a deterministic code. Serpent, the code that provided the reference results for the benchmark, is also capable of generating few-group cross-sections. However, this may both introduce a bias into any results that use those cross-sections as well as fail to evaluate the cross-section generation capability of a code that the participant wishes to use.

The process for generating the parameters for the specification itself was an iterative one. Two students were involved directly with developing the benchmark specification. The first student built the initial models and presented results to a FHR neutronics research group at UCB. The results and model were discussed and fine-tuned. The second student then replicated the model based off the specification to date. Both students used Serpent 2 for this process. The aim here was to identify any ambiguities in the specification and try to minimize the so-called "user effect". Once the results converged between the two students' models, the benchmark was then progressed to the next stage. The second student would then begin building input files for the other codes previously specified. The results from those codes would then be compared with the reference Serpent result and evaluated by the FHR research group. If required, the model parameters were tweaked until the group was satisfied that any discrepancies between results were not as a result of the specification definition.

3.3 Unit cell benchmark code-to-code comparison results

The first stage of the benchmark is based on a unit cell model of the TMSR-SF1. It is comprised of a symmetric cell containing fuel pebbles and FLiBe. The pebbles are ordered in a face-centred-cubic (FCC) lattice with a packing fraction equal to the average packing of the active region of the whole core

of TMSR-SF1. The cell contains 8 1/8ths of pebbles in each vertex of the cubic boundary and 6 ½ pebbles at each boundary face. FLiBe salt is filled in between each of the fuel pebbles. The geometry is depicted in Figure 13.

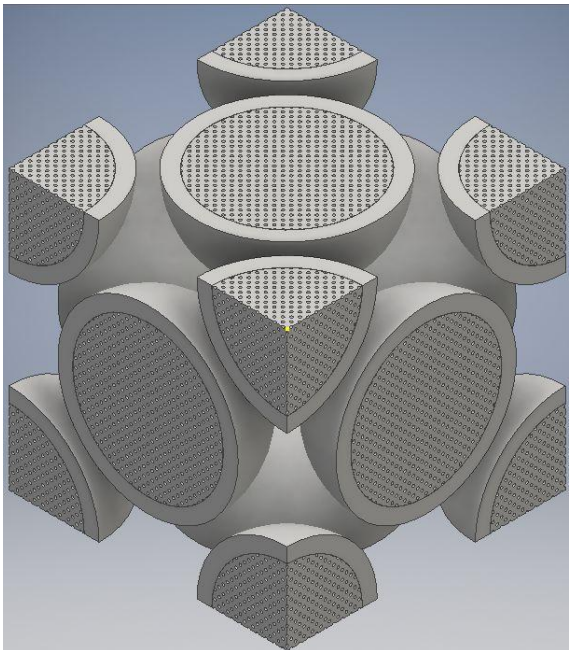

Figure 13 Geometry of fuel pebbles inside the unit cell

The fuel zone within the pebbles is also specified as an ordered FCC lattice of TRISO particles. For continuous energy Monte Carlo codes, this was explicitly modelled. For the multi-group calculations computed within a SCALE sequence, a special treatment for dealing with the double-heterogeneity was employed. Essentially, a homogenized mixture of materials is created and used in the fuelled region of a pebble during the full geometry transport calculation; the particles and graphite matrix are smeared into a single zone. The cross-sections of the materials in the homogenized mixture are adjusted via fluxes obtained from a separate transport calculation that employs a 1D geometry of a particle.
Three cases were examined in the unit cell model:

- Full volume-averaged homogenization. All geometry is collapsed into a single region and all materials blended into a single mixture. The mass fraction of each isotope is derived from the total mass of the isotope in the fully heterogeneous case divided by the total mass.
- Single level heterogeneity. The fuel zone (TRISO particles and graphite matrix) is homogenized in the fashion described above, while the pebble shell and FLiBe geometry is retained.
- Double heterogeneity. All geometry is preserved.

The figures of merit (FOM) identified for the unit cell stage of the benchmark are:

- K_{inf} – infinite multiplication factor
- β_{eff} – delayed neutron fraction
- L – prompt neutron lifetime
- Flux spectrum averaged across the whole cell (Case 3 only)
- Selected few-group cross sections (Case 3 only)

3.3.1 Case 1 – Full Homogenization

This case represents the simplest form of code-to-code validation. The model features no discrete geometry; it's essentially a point reactor model consisting of only fuel and pebbles. Table 21 contains the K_{inf} and point kinetics parameters calculated from the 5 different transport sequences used:

Table 21 Kinf, βeff and L for Case 1

Transport Code	K_{inf}	Uncertainty	Vs. Serpent [pcm]	β_{eff} [pcm]	L [μs]
Serpent 2 (MC-CE)	1.30535	± 0.00004	-	654	319
MCNP6 (MC-CE)	1.30536	± 0.00007	1	656	290
KENO-VI (MC-CE)	1.30537	± 0.00024	2	-	99.1
KENO-VI (MC-MG)	1.30802	± 0.00018	267	-	99.3/245
T-XSDRN (DO-MG)	1.30788	-	253	-	-

The kinf results generally agree with each other. The one stark contrast observable is the clustering of CE and MG results. Within each of these groups, the values are very close, but a 250-300pcm difference exists between the two of them.

The delayed neutron fraction is only available in Serpent 2 and MCNP6, though here the results are also in good agreement. Also, the prompt neutron lifetime results from Serpent 2 and MCNP are within about 10% of each other. The KENO-VI results show a much lower value, though this result is not particularly meaningful as the calculation for L did not use the adjoint flux. The KENO-VI MG result does feature an adjoint-weighted flux calculated lifetime, though this value is about 15-25% lower than the Serpent and MCNP. T-XSDRN does not feature capability to calculate either the delayed neutron fraction or prompt lifetime.

This case serves, more than anything, as a calibrating case for codes. In those terms, it would appear that a bias of a couple hundred pcm higher for MG calculations is reasonable.

3.3.2 Case 2 – Single Heterogeneity

This case is a stepping stone case between the simplest unit cell and the complex DH pebble cell. As mentioned previously, the fuel region of each pebble is blended together by volume-average homogenization, but the pebble "macro" geometry is intact. This does introduce new phenomenon into the model, such as neutron streaming between pebbles and spatial discretization of some materials, notably Li-6, a strong neutron poison. The model doesn't, however, exclude the phenomena associated with the TRISO particles; the DH is a complex structure to deal with in deterministic methodologies and it was the intention for this case to provide an additional calibration scenario for a participants results. Table 22 contains the K_{inf} and point kinetics parameters calculated from the 5 different transport sequences used:

Table 22 Kinf, βeff and L for Case 2

Transport Code	K_{inf}	Uncertainty	Vs. Serpent [pcm]	β_{eff} [pcm]	L [μs]
Serpent 2 (MC-CE)	1.34662	± 0.00004	-	656	303
MCNP6 (MC-CE)	1.34678	± 0.00007	16	647	305
KENO-VI (MC-CE)	1.34738	± 0.00019	76	-	251

KENO-VI (MC-MG)	1.34933	± 0.00020	271	-	251
T-XSDRN (DO-MG)	1.34928	-	266	-	-

K_{inf} is larger in this case when compared to the fully homogenized case, though the results relative to each to other within this case are consistent with the first case. The increased k_{inf} is likely attributed to increased neutron streaming and moderation through the graphite shells and salt. These results are consistent with IAEA-TECDDOC-1694 and [HTGR reactor physics and burnup calculations using the Serpent Monte Carlo code].

3.3.3 Case 3 – Double Heterogeneity

The final case is a unit cell with fully defined pebbles, including all the TRISO particles. In the CE codes, these particles are all modelled explicitly. In the MG codes, a treatment is used to modify the cross-sections of the fuel zone materials, then the content of that fuelled region are homogenized into a single mixture (DH cell treatment in SCALE6.1). This scenario serves as the basic simulation "building block" that closely mimics an actual salt-pebble system, albeit with the infinite pebble bed assumption. In addition to the parameters observed in the previous two cases, the flux spectrum averaged over the whole cell and selected cross sections have also been computed. Table 23 contains the K_{inf} and point kinetics parameters calculated from the 5 different transport sequences used:

Table 23 Kinf, βeff and L for Case 3

Transport Code	K_{inf}	Uncertainty	Vs. Serpent [pcm]	β_{eff} [pcm]	L [μs]
Serpent 2 (MC-CE)	1.42214	± 0.00004	-	652	277
MCNP6 (MC-CE)	1.42153	± 0.00007	-61	656	340
KENO-VI (MC-CE)	1.42163	± 0.00020	-51	-	244
KENO-VI (MC-MG)	1.42284	± 0.00017	70	-	257
T-XSDRN (DO-MG)	1.42178	-	-36	-	-

The initial comparison of k_{inf} results here looks very favorable, with the range of values about 130pcm wide and no result deviating greater than 100pcm from the reference Serpent result. However, this does not square with the results from the two previous cases between CE and MG simulations. This implies a cancellation of errors and likely a false agreement between the different codes. Furthermore, the values obtained from Serpent and MCNP start to deviate, an unexpected result. This could be attributed to different thermal scattering data used between the two codes; although the ENDF/B-VII.0 cross section data and TSL was used in all simulations within this exercise, the specific instances packages with, at least, Serpent and MCNP may be different.
Figure 14 shows the scalar flux spectrum, divided into 238 energy groups (SCALE-238 group structure) for each of the codes in the DH case:

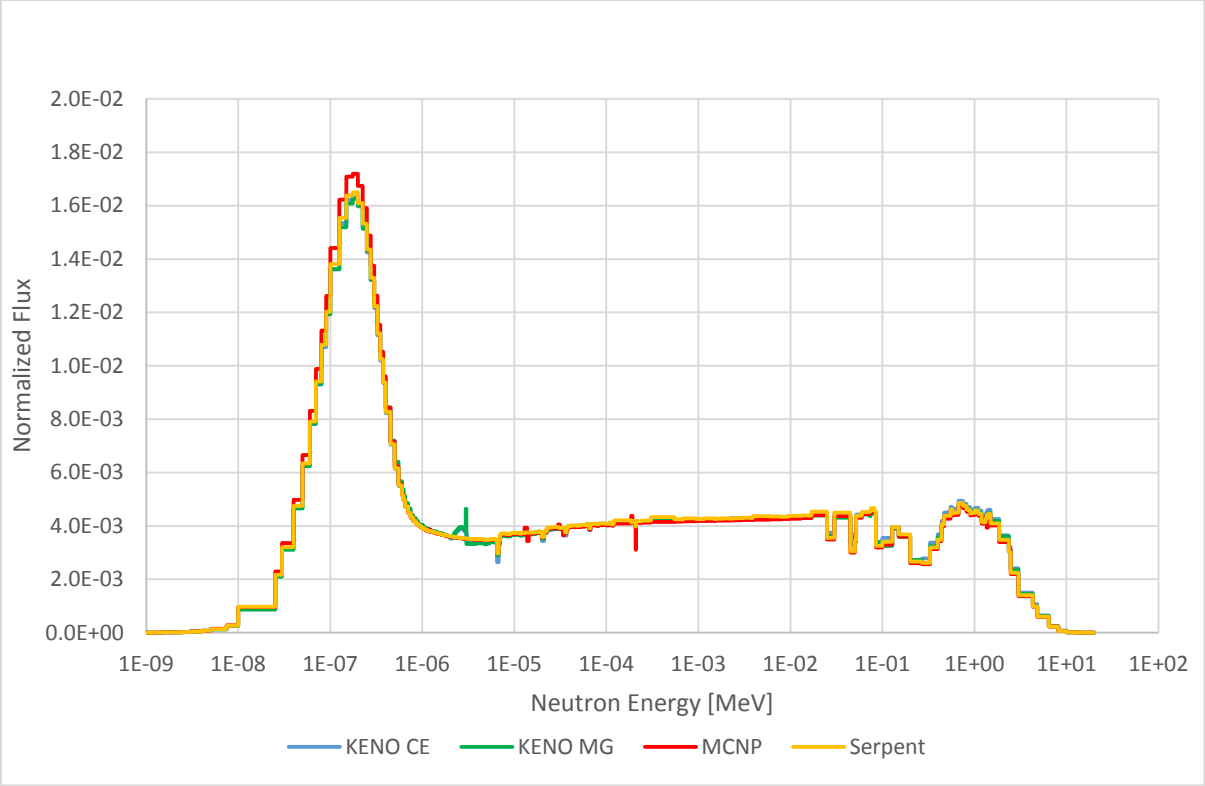

Figure 14 Neutron flux per lethargy as a function of neutron energy for Serpent 2, MCNP6 and KENO-VI

Between each of the Monte Carlo codes there is good agreement in the spectral data, upon visual inspection. There is a small artefact between the two KENO data and the others: a short, broad peak in the epithermal region, for example. After some discussion, no consensus was arrived at for this aberration, though a recheck of the energy group definition would be done. The one serious discrepancy is the MCNP vs. the other Maxwellian peak, which is higher than the rest. This also could be a result of inconsistent TSL data used for graphite between each code.

3.4 3D full core benchmark code-to-code comparison results

The second stage of this benchmark specification is a simplified model of the TMSR-SF1 core. The core is filled with FLiBe salt and fuel pebbles. The coolant inlet to the core is at the bottom, where coolant flows upwards through the pebble bed and exits via the outlets at the top of the system. The top and bottom reflectors of the core are graphite truncated conical sections, providing converging and diverging flow of coolant and pebbles at the top and bottom, respectively. The active region is radially surrounded by a graphite reflector. An axial view of the TMSR-SF1 core is shown in Figure 15.

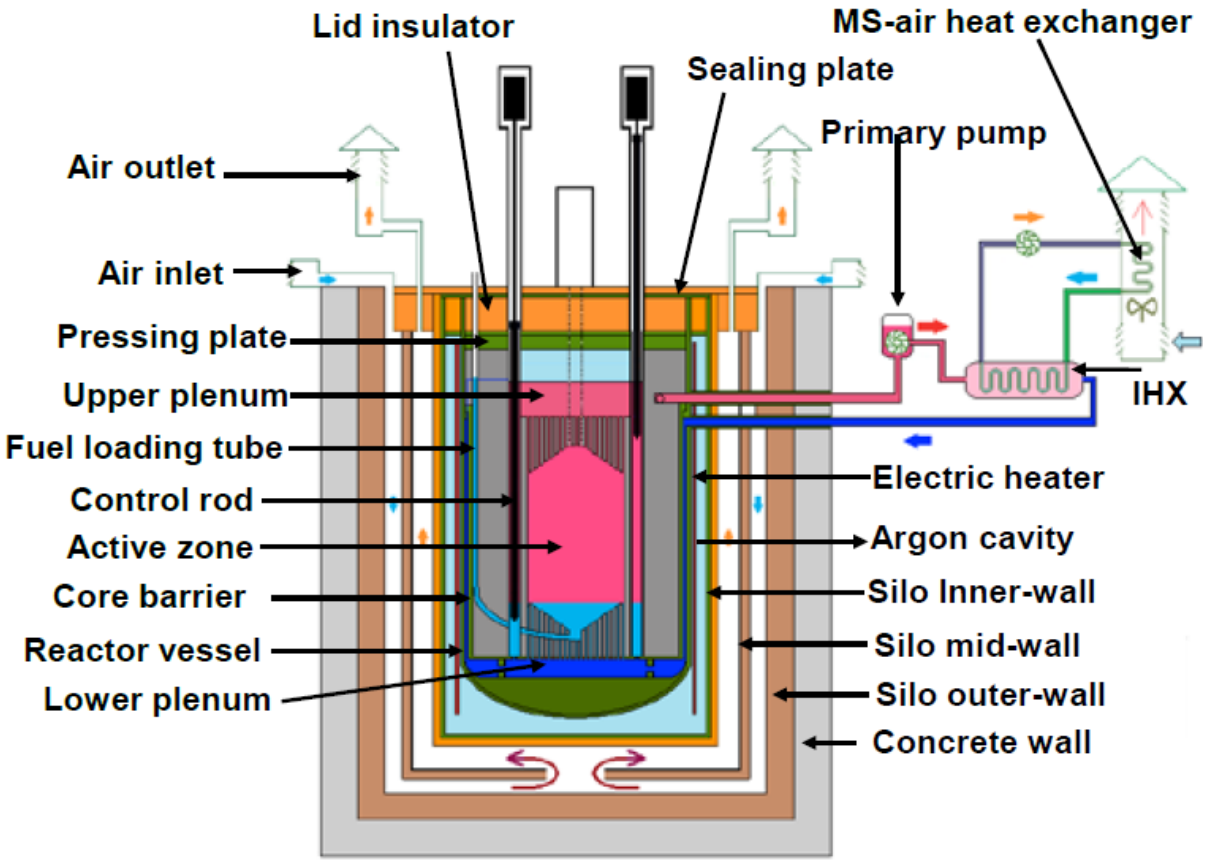

Figure 15 Axial section view of the TMSR-SF1

The model used in the benchmark cuts away all the structure and components outside of the core vessel, and then simplifies the geometry considerably. Essentially, there are 5 regions of interest in the model:

- Active/fuelled region – This is filled with a 3D lattice of the unit cell from the first stage of the benchmark. All the fuel for the model is contained in this region.
- Salt region – Below the active region is a section of the core filled with just FLiBe salt.
- Top reflector – This is a solid cylindrical section composed of a volume-averaged mixture of graphite and FLiBe salt. Rather than explicitly modelling the conical section of the top of the reflector vessel, which is difficult for some codes to achieve, a reasonable compromise was to blend the discrete zones of graphite and salt together into a single region.
- Bottom reflector – essentially the same as the top reflector.
- Radial reflector – Annular cylinder composed of graphite.

There are a few other discrepancies to acknowledge. Rather than modelling any control elements into the design, the number of pebbles loaded into the core was iterated until criticality was achieved. The model includes 7168 pebbles, the number required to achieve criticality using a random packing with a fresh core and no control elements. The pebble ordinates were determined using discrete element modelling (DEM) software to achieve a reasonable packing configuration for a pebble bed. The nominal pebble configuration was calculated, resulting in a packing factor lower than specified in the benchmark (and by the figure quoted in TMSR-SF1 design documents). Consequently, the pebble bed was "shaken" until the bed compacted to a packing factor of 57%.

Rather than using explicitly defined pebble locations, a regular lattice of the FCC arrangement from in Stage 1 was used. The size of the fuel region was implemented in the model based on the approximate dimensions of the space the pebbles occupied in the DEM simulation, then the fuel volume was calculated stochastically. Due to the regular lattice, the pebbles on the periphery of the core were cut and the exact fuel volume was not known. The pitch of the particle lattice was first tweaked so that the effective particle packing factor was maintained. Following that, the pitch of the pebble lattice was iterated to preserve the nominal pebble packing factor. As such, it should be noted that the lattice used in the unit cell and the simplified core model are very similar, but not identical.

This scenario is far from an actually deployable state for the TMSR-SF1, but suitable due to its simplicity for this benchmark exercise. Furthermore, as the specification uses an ordered packing of pebbles, the packing factor is constant over the whole fuel region. In a random packed bed, the packing is tighter away from the wall and looser at the wall. This difference does impact the FOM expected from the benchmark. For example, keff is lower in the ordered packing case when compared to the random packing, presumably from the regular neutron streaming between pebbles, and thus potentially increasing the leakage of the system.

Another point to mention is that the conical converging section of the core/reflector at the top of the active region is also populated with pebbles in the TMSR-SF1 design. This model ignores this by just substituting the entire conical section with a volume-averaged homogenized cylindrical section of graphite and FLiBe. This may lead to a lower top leakage in the benchmark model than may be true of the TMSR-SF1. Nevertheless, it should be reiterated that this is a simplified benchmarking exercise for code-to-code verification, rather than a high-fidelity analysis of the TMSR-SF1.

The figures of merit (FOM) identified for the simplified core stage of the benchmark are:

- K_{eff} – effective multiplication factor
- β_{eff} – delayed neutron fraction
- L – prompt neutron lifetime
- Flux spectra
- Axial and radial thermal neutron flux profiles
- Power Distributions
- Reactivity Coefficients
- Neutron Leakage

3.4.1 Multiplication Factors and Point Kinetics

Unlike the unit cell case which was an infinite lattice of pebbles, this scenario has finite bounds. The outer boundaries of the reflector regions are all subject to black boundary conditions. This also introduces a non-zero leakage into the system. At present, work as only been carried out on this stage of the benchmark using MC codes. Table 24 contains the K_{eff} and point kinetics parameters calculated from the 4 different transport sequences used:

Table 24 Kinf, βeff and L for Stage 4

Transport Code	K_{eff}	Uncertainty	Vs. Serpent [pcm]	β_{eff} [pcm]	L [μs]
Serpent 2 (MC-CE)	0.99338	± 0.00008	-	679	667
MCNP6 (MC-CE)	0.98945	± 0.00008	-393	670	672
KENO-VI (MC-CE)	0.99047	± 0.00020	-291	-	622
KENO-VI (MC-MG)	0.99889	± 0.00023	551	-	702

3.4.2 Neutron Flux Profiles

One interesting feature of such a compact reactor with a large portion of moderating facility located in a reflector is the two distinct “humps” in the radial thermal flux profile. At the center of the core, where the power density is high, there is a maximum in the thermal neutron flux. Around 10cm into the radial reflector from the inner diameter is a second, narrower hump in the flux. Obviously capturing this result in a code is important and was considered to be a suitable FOM for participants to obtain.
Figure 16 shows the radial neutron flux profile as calculated by Serpent 2 and MCNP6.

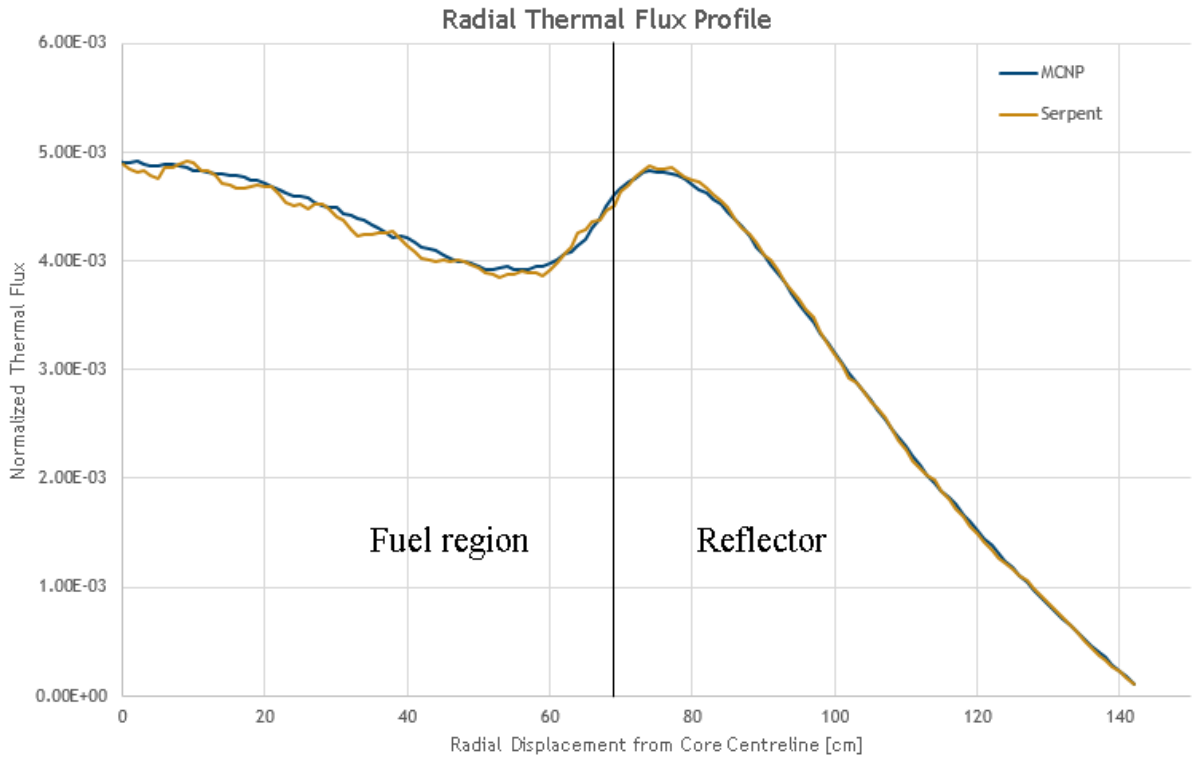

Figure 16 Radial thermal neutron flux of the Stage 2 model. Flux is sampled at 0.5cm intervals radially. Each interval averages the flux axially over the whole height of the fuel zone

A similar double peak of thermal flux is observed axially through the centerline of the core. The first peak is seen near the center of the fuelled zone and the second just inside the top reflector. It should be noted that the top reflector region in the model is not accurately representative of the actual geometry of TMSR-SF1, but is nevertheless a useful system feature to try and capture for the purposes of verification. Figure 17 shows the axial thermal neutron flux profile of the core as simulated by Serpent 2 and MCNP6.

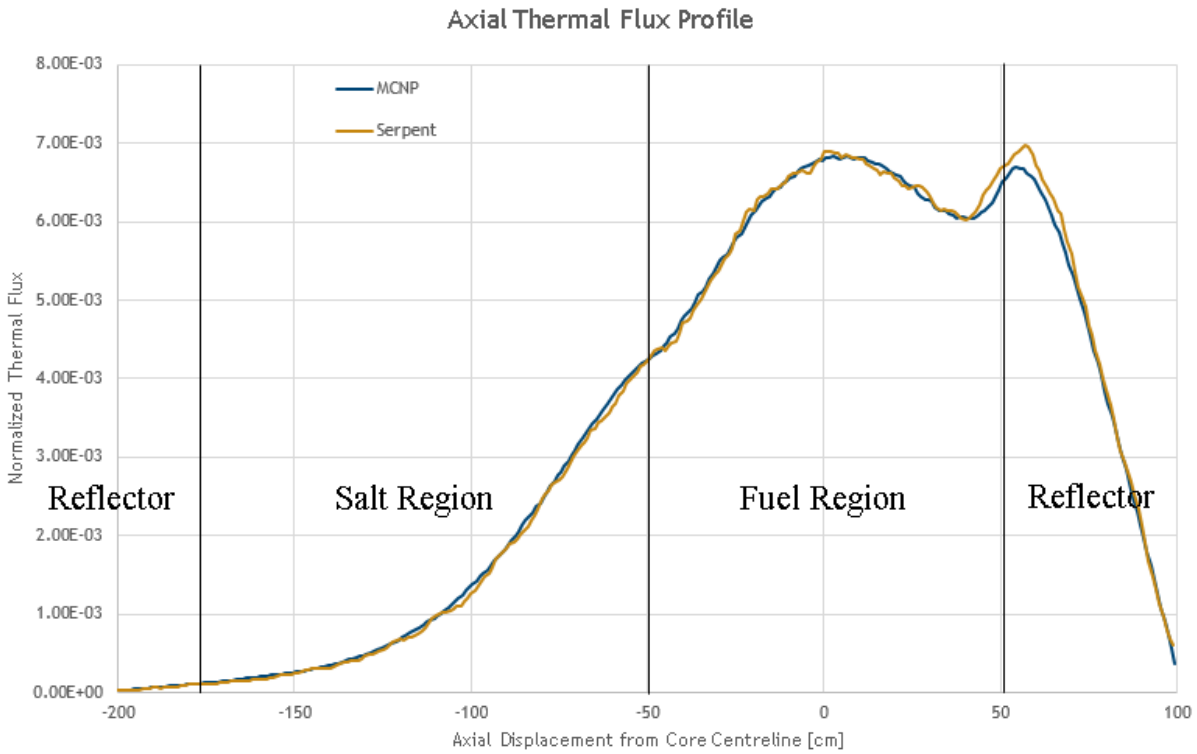

Figure 17 Axial thermal neutron flux of the Stage 2 model. Flux is sampled at 0.5cm intervals axially. Each interval averages the flux radially over the whole of the fuel zone

Some discussion was given to determining power peaking factors. First, contrary to a typical light-water reactor (LWR) which are largely axially prismatic, the TMSR-SF1 is highly heterogeneous in fuel geometry. As a result, the axial and radial power peaking factors are disjunctive and a traditional approach might not be as useful. Table 25 contains the results from this traditional approach calculated using Serpent 2 and MCNP6.

Table 25 Power Peaking Factors in the Simplified Core

Code	Axial Peaking Factor	Radial Peaking Factor
Serpent 2	1.1479	1.1106
MCNP6	1.1314	1.1236

A more useful data may be to locate the pebble or region with the highest power density. Nevertheless, looking at the thermal flux profiles and assuming that core power is proportional to the thermal flux, the results in Table 25 looks reasonable.

3.4.3 Reactivity Coefficients

The final FOM considered for the simplified core model are selected reactivity coefficients (RC): coolant, void and fuel Doppler coefficients. The coolant RC is the temperature dependence of the salt reactivity contribution. Both the cross-section temperature and corresponding density variation is included in the calculation. The void coefficient was calculated by changing the density of the salt alone. The Doppler RC was calculated by varying the cross-section temperature of the uranium cross sections. The temperature-dependent RCs were determined using 50K intervals over a 300K range of 900K to

1200K. The void RC was determined using 2% void intervals between 0 and 10% reduction of salt density. Table 26 contains the specified RCs calculated using Serpent 2, MCNP6 and KENO-VI.

Table 26 Reactivity Coefficients

Code	Coolant (pcm/K)	Void (pcm/%)	Doppler (pcm/K)
Serpent 2 (MC-CE)	-1.630 ± 0.033	-13.73 ± 0.99	-2.160 ± 0.033
MCNP6 (MC-CE)	-1.680 ± 0.039	-11.30 ± 1.13	-2.160 ± 0.038
KENO-VI (MC-CE)	-1.557 ± 0.092	-8.70 ± 2.90	-2.083 ± 0.094
KENO-VI (MC-MG)	-1.763 ± 0.108	-15.00 ± 3.25	-

A comparison of these values shows that Serpent and MCNP6 are in good agreement with each other, but the KENO-VI results varying significantly. It should be noted that there is greater uncertainty associated with the KENO RCs and the results were obtained from non-adjoint-weighted calculations.

3.4.4 Neutron Leakage

The leakage values were obtained by creating neutron flux surfaces tallies at the outer boundary of the top, bottom and radial reflectors.

Table 27 Leakage from top, bottom and radial reflectors

Code	Neutron Leakage		
	Top	Bottom	Radial
Serpent 2	-11.46%	-0.16%	-5.68%
MCNP6	-11.60%	-0.16%	-5.71%

4 Recommendations for future work

Based on the work presented here and the discussions that took place during the April 2016 FHR workshop at UCB, there are a number of research avenues that can be pursued. The most obvious direction is the current one: to finish the in-house code-to-code verification. This serves both to offer some assurance on the robustness of the specification as well as providing a reasonably credible baseline for comparison of future results from other codes. It should be stressed that this baseline of comparison contains no pretense of being objectively correct, but merely strives to offer additional sample points for a given FOM and a basis for intuition for researchers.

4.1 Recommendations following the April 2016 Workshop

In parallel with completing the specification within the scope defined, the feedback received from the workshop should be incorporated into the existing and planned specification design. Such feedback includes:

- Using SCALE6.2, now released, in place of SCALE6.1. This provides new functionality as well as a new 252-group structure, which may provide higher fidelity results.
- Using adjoint weighting where possible. The balance of the KENO results presented here, adjoint weighting was not used in the transport sequence.
- Relax some of the constraints of the specification to allow participants more room to conduct the benchmark in a manner that they deem suitable. While this may limit some of the comparison power when aggregating the results, it will provide a wider range of capability comparison. In addition, by allowing more freedom in how to conduct the benchmark, user incentive to participate and complete the benchmark should be higher. This does require a rigorous reporting system to compliment all results with the methodologies used to obtain them.
- Reduction of some of the FOM. For example, the complete suite of cross-sections specified in the unit cell case may be excessive and largely not useful. Reducing the number of cross-sections to a few key instances would be preferable, such as the resonance group for U-238 radiative capture.
- Quantification of S(a,b) influence on key results using each of the different codes. It was suggested that specific instances of a given evaluation may differ depending on which codes the nuclear data was packaged with. The S(a,b) data may also be used to treat the cross-sections differently. This is a useful phenomenon to quantify.
- Though the benchmark does not serve to provide a rigorous basis for analysis of FHR systems themselves, modelling a system that is a reasonable representation of a design (e.g. TMSR-SF1) is still preferable. Following this logic, the Li-7 enrichment should be increased to 99.995% from the 99.99% used in the work done to date.
- Adding a fission density FOM to the simplified core benchmark as a function of r and h. This might be an interesting expansion on the power peaking factor. This would be more complex to implement in the specification as a careful selection of how that data was obtained would need to be considered, owing to the heterogeneous location of fuel throughout the core. This FOM was included in the GT neutronics PIRT for plate-type fuel.
- Looking at the CENDL data available for TMSR-SF1 materials.

- Looking at the new evaluation of a S(a,b) treatment for FLiBe salt.
- Inclusion of the code DRAGON as a deterministic code comparison.
- Use MCNP in MG mode to offer another basis for MG comparison.

4.2 Path Forward for Benchmarking

The scope for the current benchmark is set and there is consensus that it is appropriate, but more benchmarking should be conducted following the conclusion of this work. This next step will likely include examining burnup and control rod reactivity worth. Initially these were considered for inclusion into the current benchmarking effort, but it was generally received that the confidence in codes for simpler, more fundamental aspects of reactor simulation should be quantified first. Furthermore, an appropriate approach and methodology for simulating FHR systems will likely emerge from the lessons learned from this benchmark, eliminating some sources of error in future work and reducing the amount of iteration required to build a new benchmark specification, particularly given the high computational cost of MC codes combined with the sheer number of unique calculations that are required for both burnup and control rod worth.

Control rod worth should be a relatively straightforward exercise to complete, particularly given the approximate symmetry of the system. Burnup, on the other hand, will require some thought in how to: discretize the fuel, determine the time steps and, if deemed necessary, migrate the pebble or fuel compositions throughout the core. Some scoping and sensitivity work should be conducted using high-fidelity codes, such as Serpent and MCNP, to determine the best course of action.

5 TMSR project overview

TMSR project was started in 2011, involving two types, the solid-fueled thorium-based molten salt reactor (namely the FHR, TMSR-SF) and the liquid-fueled thorium-based molten salt reactor (TMSR-LF). The purpose of this project is to develop the thorium-based nuclear energy system with a variety of functions such as power generation, spent fuel burn-up, application in arid regions, small module application and hydrogen production.

5.1 TMSR-SF1 Design Overview

5.1.1 Design considerations

The goal of TMSR-SF1 project is to build the first thorium-based solid-fueled molten salt reactor in the world and achieve system integration, key technology and experience for the next demonstration reactor. The technical goals including: 1) Obtaining the ability of the reactor physics design, the thermal hydraulic design, the security system design and the engineering design for the solid-fueled thorium based molten salt reactor. 2) Processing the ability of reactor integration, construction, operation and maintenance. 3) Verifying the reactor physics, thermal-hydraulic behavior and security features of the solid-fueled thorium based molten salt reactor. 4) Verifying the service behavior of the materials, fuel, molten salt and equipment of the solid-fueled thorium based molten salt reactor.
Since TMSR-SF1 is the first experimental reactor in the world, the design considerations are as follows: (1) Use existing technology if possible; (2) Large design margin to keep safe; (3) Simplified core design. Figure 18 shows the layout of the reactor, Figure 19 shows the schematic diagram for TMSR-SF1 reactor, and Table 28 shows the TMSR-SF1 major parameters.

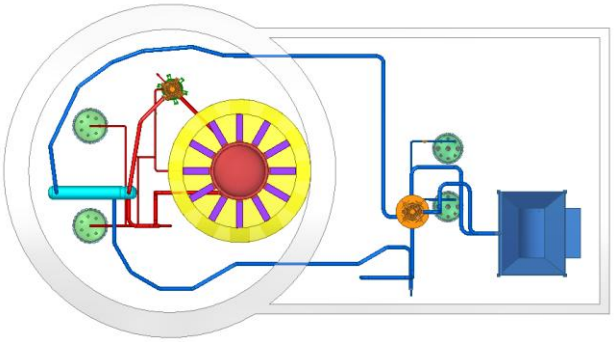

Figure 18 Layout of TMSR-SF1

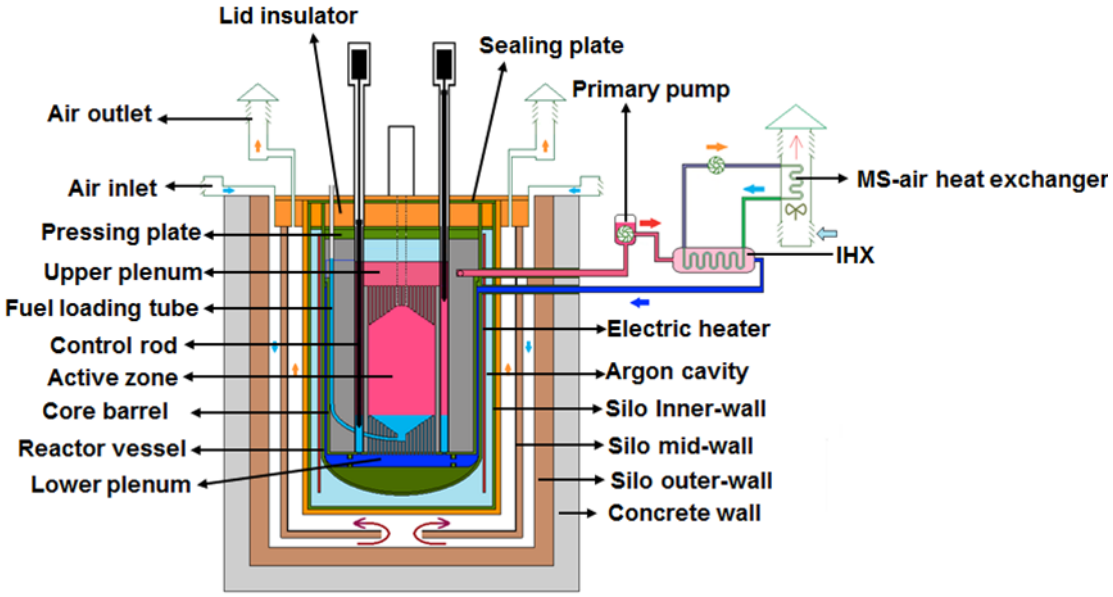

Figure 19 Schematic of the TMSR-SF1

5.1.2 Main features

Here is the overview of TMSR-SF1:

1) Reactor power: the nominal designed power is 10 MWt. It contains about 15000 fuel pebbles and graphite pebbles when fully loaded.

2) Fuel elements: the pebbles loaded in the high temperature gas cooled reactor are used in TMSR-SF1. The maximum fuel temperature limit is 1200 ºC under the normal operation condition.

3) Coolant: the 1st loop coolant is 2LiF-BeF_2 with ^{7}Li enrichment 99.99 %. The 2nd loop coolant is LiF/NaF/KF molten salt.

4) Core: it includes active core, reflector and core barrel. The fuel is arranged randomly and inlet temperature of coolant is 600 ºC, outlet temperature of coolant is 650 ºC.

5) Reactivity control: control rod system is used to realize the functions such as temperature control, power regulation, burn-up compensation and shutdown. Type I control rods is used as the first shutdown system, and control II rods with molten salt drain tank is used as backup shutdown system.

6) Loop system: Loop system includes the 1st loop, the 2nd loop, gas loop and molten salt detecting facilities and so on.

7) Residual heat removing system: Using the loop under normal condition and using core containment passive heat dissipation in the loss of flow accident.

8) Pebbles loading and discharging: pebbles are loaded one by one from the bottom of the core by buoyancy and discharged from the channel at the top of the core.

9) Material: Hastelloy-N is used for reactor vessel, in-core structure and loop. Graphite is used as reflector. SiC/SiC composite material or C/C composite material is used for control rod sleeve.

10) Safety facilities: including containment, passive residual heat removal system and so on.

Table 28 TMSR-SF1 major parameters

Parameters	Value
Thermal power	10 MW
Life-time	20 yr
Coolant outlet temperature	650 °C
Coolant mass velocity	84 kg/s
Cover gas pressure	0.05 MPa (abs.)
Fuel Elements	Pebble diameter 6 cm Uranium enrichment 17.0 % Boron equivalent < 4.0 ppm
Primary Loop Coolant	LiF/BeF_2(mol%): 2:1 Li-7abundance >= 99.99 % Boron equivalent < 2.0 ppm
Reactor	Graphite density 1.825 g/cm^3 Boron equivalent < 1 ppm
Metal material in reactor	UNS -N10003
Control rods	The first set: 2 regulating rods, 8 compensation rods, 3 shutdown rods Backup: 3 shutdown rods with molten salt drain tank
Primary pump	Vertical cantilever centrifugal pump
Heat exchanger	U type pipe molten salt/molten salt heat exchanger, Straight pipe molten salt/air heat exchanger
Residual heat removal	Active and passive method Passive residual heat removal fraction: 2 %
The 2^{nd} loop Coolant	LiF/NaF/KF (mol%): 46.5 / 11.5 / 42.0 Flow rate: 150 kg/s

TMSR-SF1 core consists of active region, reflector, core support mechanism, core barrel, reactor vessel, reactor container, control rods, reactor measuring mechanism, etc. The active region surrounded by reflector consists of upper and bottom truncated cones, and the middle cylinder. The diameter of the cylinder is 135.0 cm, and the height is 180.0cm. The minimum diameter and height of the upper and lower circular truncated cones are 30.0 cm and 30.3 cm respectively. The angle between the cones and the horizontal plane is 30 degrees. The pebbles, including about 13000 fuel pebbles in the upper zone and graphite pebbles filling the rest room, are randomly distributed in the active zone. The packing fraction of pebbles is 60 %. The reflector consists of upper, lower and side reflector. The external diameter of graphite reflector is 285.0 cm and the height of reflector is 300.0 cm. The side reflectors around the active core host channels for neutron sources and measurement equipment which are shown in Figure 20. TMSR-SF1 core channels include sixteen control channels, one neutron source channel, two physical start-up detector channels, seven neutron flux density distribution measurement channels, six temperature measurement channels, two fuel pebble injection channels, one molten salt loading and unloading channel, three material irradiation experiment and surveillance channels and two standby channels.

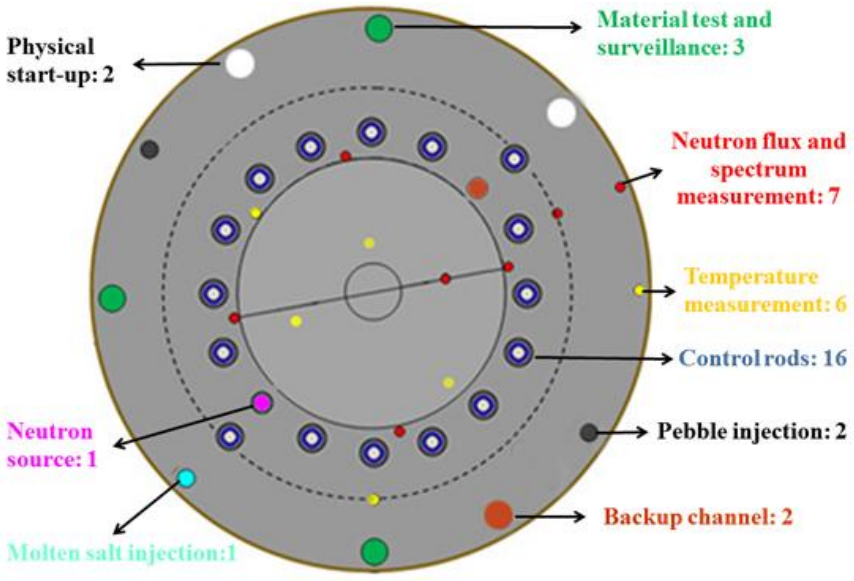

Figure 20 TMSR-SF1 core channels layout diagram

5.2 TMSR-LF1 Design Overview

Considering the huge challenges, the technical and construction goals for a 2 MW liquid-fueled thorium molten salt reactor (TMSR-LF1) are as follows: Build a 2 MW liquid-fueled MSR (TMSR-LF1); Gain experiences of design, construction and operation; Obtain tests on reactor physics, components and safety issues; Validate circuit, materials and irradiation experiments; Validate key techniques of reprocessing flowsheet, fluorination volatilization and vacuum distillation; Validate Th-U conversion and online refueling; Provide key test data for the feasibility of future large-scale TMSR-LFs development (fuel salt preparation, structure materials etc.).

5.2.1 Design considerations

The guiding considerations in the design of TMSR-LF1 can be classified under the headings of “reactor design”, “pyroprocess”, and “Th-U”. The term of “reactor design” includes several aspects, which are the design and construction of test reactor with liquid fuel salt, research on key technical equipment, system integration, critical physical experiments and investigation on operation stability, safety and controlling of TMSR-LF1 under conditions of online refueling, continuous gas removing and online reprocessing. The notation of “pyroprocess” contains the thermal test of technological process of pyroprocessing, the required process conditions for thermal verification of Th-U fuel cycle, the ability of fuel salt online reprocessing, the validation on equipment dependability, process stability and measurement of accessibility of fluorination volatilization and vacuum distillation. The expression of “Th-U” represents the operation with thorium-uranium mixture fuel and online pyroprocessing, the verification experiment of Th-U conversion, evolution of importance nuclides and online refueling.

5.2.2 Main features

According to the technical and construction goals, TMSR-LF1 is designed to have the experimental feature and ensure the safety and engineering feasibility. The schematic diagram of main systems is given in Figure 21**Error! Reference source not found.**, including nuclear power system, heat transfer system, control and measurement system, pyroprocessing system, tritium removal system, security system and auxiliary system.

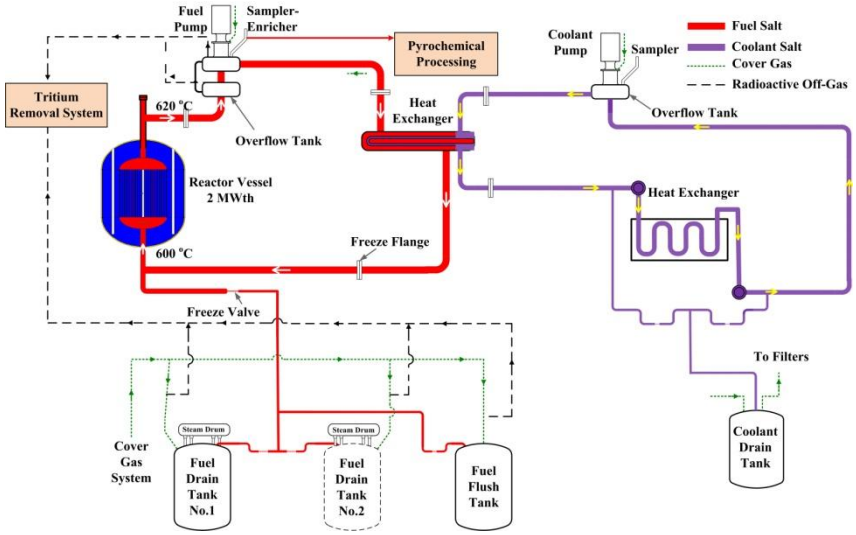

Figure 21 TMSR-LF1 flowsheet

The nuclear power generated in reactor core is transferred to heat exchanger through primary loop, and then it is released to air by air radiator in the secondary loop. The reactor core of TMSR-LF1 is a single-region, graphite-moderated, graphite-reflected, fluid-fuel type of reactors with a design heat generation of 2 MW. The circulating fuel salt is mixture of lithium and beryllium fluoride salts that contains thorium and uranium fluorides. Reactor heat is transferred from the fuel salt to a similar coolant salt and is then dissipated to the atmosphere. The average temperature for fuel salt, the temperature limitations for structural materials and the reactor vessel pressure limitation are about 610 ºC (lower than the boiling point of 1400 ºC), 704 ºC and less than 5 atm, respectively.

The core design principles for TMSR-LF1 are as follows: low amount of uranium loading and U-235 enrichment less than 20%; Li-7 abundance is set to be 99.95%; appropriate amount of thorium for the verification of Th-U fuel cycle; lower excess reactivity benefited from online refueling; negative temperature feedback; simplified core design for the integration, construction, operation, controlling and maintenance; consideration on the uncertainty of physical parameter, the engineering feasibility and practical ability of post-processing technology.

Figure 22 shows the layout scheme of the reactor. The reactor vessel contains the graphite-moderated core and its supporting plate, the graphite reflector, the upper and bottom plenums, and the inlet/outlet pipes. Outside of the reactor vessel is thermal insulation layer with a thickness of 0.5 m, which is made of chamotte brick. Outside of the insulation layer is a closed silo (with air in it) with a gap of 0.5 m. Outside of the silo is another thermal insulation with thickness of 0.8 m and a concrete wall with thickness of 0.7 m. The thermal insulation design of the reactor vessel ensures the total heat loss of the reactor during normal operation at 2 MW is 2.6 kW.

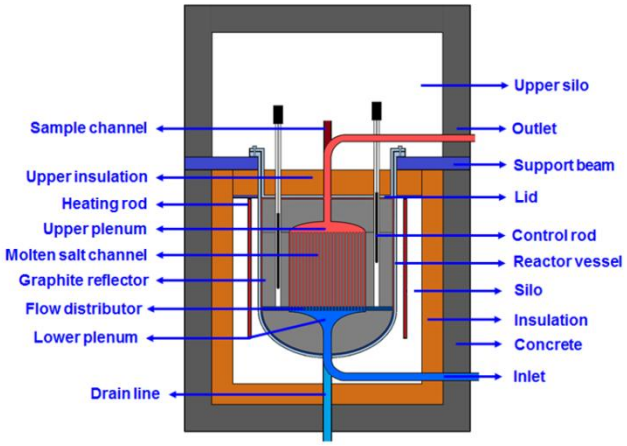

Figure 22 Schematic of the TMSR-LF1

The reactivity control system of TMSR-LF1 consists of control rods, including regulating rods, a shim rod and a safety rod, and fuel salt drain tank. Some of the rods compose the first shutdown system, while the left rods together with the fuel salt drain tank compose the second shutdown system. The above two different shutdown systems can satisfy the requirements of diversity and avoid the common cause failures with different drive mechanism principle.

The major thermal-hydraulic characteristics of TMSR-LF1 consists of two loops to transfer nuclear energy from reactor core to ambient during normal operation and shutdown and passive ways to drain fuel from reactor core and remove residual decay heat to ambient during emergency. TMSR-LF1 adopts a single fluid pathway design of thermal-hydraulic (Figure 23). There are two sets of heat transport system with forced convection including the primary cooling loop and IHX (FLiBe+UF+ThF) and the secondary cooling loop and IHX (FLiNaK). Besides, there are two sets of residual heat removal systems including a normal residual heat removal system with forced convection (heat exchanger) and a passive residual heat removal system with natural convection (emergence drain tank).

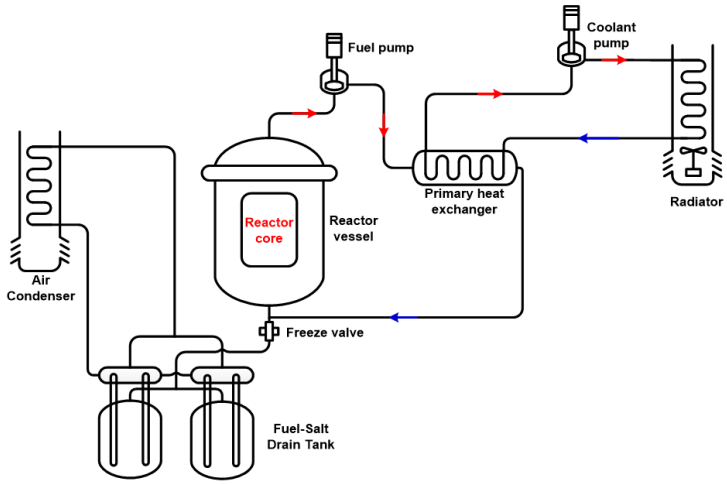

Figure 23 Thermal-hydraulic system flow scheme of TMSR-LF1

5.2.3 Fuel salt and materials

The fuel salt has a low cross section for the parasitic absorption of neutrons, and when used with nuclear-grade graphite as the moderator, very good neutron economies can be achieved. Molten-salt reactors are thus attractive as highly efficient converters and breeders on the Th-U fuel cycle. The fluoride salts used as the fluid fuel mixture have good thermal and radiation stability and do not undergo violent chemical reactions with water or air. Taking into account operating temperature, compatibility, proficiency of manufacture process and operating experience of fuel salt, TMSR-LF1 project adopts quaternary molten fluoride salts (LiF-BeF2-ThF_4-UF_4). Beryllium fluoride is used to obtain a low melting point. Lithium fluoride (99.95% ^{7}Li in both fuel and coolant salts) imparts good fluoride properties to the mixture. Fuel salts containing thorium are of interest for future large-scale breeder reactors. As a test reactor, TMSR-LF1 will be operated with low enriched uranium (<20%) and a certain amount of thorium for the validation of Th-U fuel cycle. In order to ensure chemical purity of fuel salt, reactor core and primary loop should be purged by flushing slat. Furthermore, coolant salt (LiF-NaF-KF) in the secondary loop is required to be chemically compatible with fuel salt.
Materials include the structural materials, neutron moderator and/or reflector. Structural materials are used to fabricate the reactor vessel, loops, control rod sleeves, which should have long-term stable properties and enough strength and ductility in multiple extreme environments e.g. high temperature (T>650 ºC), corrosion of fuel salt and high neutron flux radiation. UNS N10003, such as GH3535 alloy made in China, is a candidate structural material for TMSR-LF1. Although UNS N10003 has been proved to have excellent resistance to fluoride salt in MSRE, it has not been qualified in ASME code yet. Neutron moderator and/or reflector must have high purity, high density and isotropy as well as excellent resistant to neutron radiation and fuel salt corrosion or low permeation. Nuclear-grade graphite is selected as the neutron moderator and reflector for TMSR-LF1. Although there are several kinds of candidate nuclear-grade graphite in the world market, the nuclear-grade graphite produced in China is preferred to guarantee the reliable supply, low cost and short delivery cycle.
Additionally, the most important issues of materials TMSR-LF1 include the supply of materials and their preparation, processing, welding and qualification in ASME code.

5.2.4 Safety considerations of TMSR-LF1

The basic safety functions of TMSR-LF1 include the control of reactivity, removal of decay heat and containing radioactivity. Enough large negative temperature coefficients of the reactor and the low excess reactivity are such that the nuclear safety is not primarily dependent upon fast-acting control rods. The safety considerations of TMSR-LF1 are the containment requirements, fuel drain system, long term storage of the irradiated fuel salts, safety impacts of separation process, and reference cases for the TMSR-LF1 licensing.
The major barriers of the radioactive release, including the primary coolant and cover gas system boundary, containment vessel and reactor building, are used to contain radioactivity. The fuel drain system is a classical solution through which the fuel salt flows to a drain tank via a freeze valve during reactor shutdown and decay heat removal. The long term storage of the irradiated fuel salts needs a long term safety concern and may be required for project approval and licensing. Thus, the intermediate storage of irradiated fuel salts may be practical and necessary, in which the irradiated fuel salts may not be able to keep in molten state for all time, and continuously monitoring is necessary. The major separation process includes the gases extraction of Xe, Ke, tritium, etc. and separation of actinides and FPs. Accumulating radioactive isotopes from treatment may results in the risk of accumulated isotopes release. Large amount of actinides and FPs out of the reactor need a new and complex reprocessing facilities.